Disentangling cosmic-ray and dark-matter induced γ-rays in galaxy clusters

D. Maurin[1], C. Combet[1], E. Nezri[2], and E. Pointecouteau[3,4]

[1] Laboratoire de Physique Subatomique et de Cosmologie, Université Joseph Fourier Grenoble 1/CNRS/IN2P3/INPG, 53 avenue des Martyrs, 38026 Grenoble, France
e-mail: dmaurin@lpsc.in2p3.fr

[2] Aix Marseille Université, CNRS, LAM (Laboratoire d'Astrophysique de Marseille), UMR 7326, 13388 Marseille, France

[3] CNRS, IRAP, 14 avenue Edouard Belin, 31400 Toulouse, France

[4] Université de Toulouse, UPS-OMP, IRAP, 31400 Toulouse, France

ABSTRACT

Context. Galaxy clusters are among the best targets for indirect dark matter detection in γ-rays, despite the large astrophysical background expected from these objects. Detection is now within reach of current observatories (*Fermi*-LAT or Cerenkov telescopes); however, assessing the origin of this signal might be difficult.

Aims. We investigate whether the behaviour of the number of objects per "flux" bin ($\log N - \log F$) and that of the stacked signal could be used as a signature of the dominant process at stake.

Methods. We use the CLUMPY code to integrate the signal from decaying or annihilating dark matter and from cosmic rays along the line of sight. We assume the standard Navarro-Frenk-White (NFW) profile for the dark matter density and rely on a parametrised emissivity for the cosmic-ray component. In this context, the consequences of stacking are explored using the MCXC meta-catalogue of galaxy clusters.

Results. We find the value of the slope of the $\log N - \log F$ power law (or the increase of the signal with the number of stacked objects) to be a clear diagnosis to disentangle decaying dark matter from cosmic-ray induced γ-rays. For dark matter annihilation, depending on the signal boost from the substructures, it is either similar to the cosmic-ray signal (no boost) or similar to the decay case (large boosts). The shift between the brightest object and its followers also depends on the signal origin. For annihilation, this shift and the stacked signal are poorly constrained because of the large uncertainty affecting the boost. We also underline that the angular dependence of the annihilation signal is not universal because of the substructure contribution.

Key words. astroparticle physics – galaxies: clusters: general – gamma rays: galaxies: clusters – dark matter – cosmic rays

1. Introduction

Contamination by astrophysical backgrounds is the curse of dark matter (DM) indirect detection searches. Ways around this issue are multi-wavelength (Regis & Ullio 2008) or/and multi-messenger (Pato et al. 2009) analyses. In γ-rays, background-free objects such as dwarf spheroidal galaxies (dSphs) are another option (Walker et al. 2011). For targets presenting an astrophysical background, a useful diagnosis comes from the spectral behaviour, which differs for DM-induced or cosmic-ray (CR)-induced γ-rays: DM signals should exhibit a sharp cut-off at the DM mass (Bringmann et al. 2011), whereas astrophysical processes produce power laws with a slope $\sim 2-3$ (the cut-off energy depends on the source). For instance, the Galactic centre signal observed by the High Energy Stereoscopic System (H.E.S.S., Aharonian et al. 2004) is consistent with astrophysical sources. Despite their astrophysical background, galaxy clusters are also promising DM targets in γ-rays (or at radio and microwave frequencies) as first proposed in Colafrancesco et al. (2006). Cerenkov instruments have set constraints on a DM signal or astrophysical background from the non-detection in several of these objects: Perseus and Abell 2029 from Whipple (Perkins et al. 2006); Abell 3667 and 4038 from Kangaroo (Kiuchi et al. 2009); Coma, Abell 496 and 85 from H.E.S.S. (Aharonian et al. 2009a,b). A broader survey has been

made by the *Fermi*-LAT instrument, where 33 (resp. 49) clusters were analysed in Ackermann et al. (2010) (resp. Ando & Nagai 2012). The consequences for hadronic models are discussed, e.g. in Jeltema & Profumo (2011). Recently, a detection was reported by the MAGIC collaboration in the Perseus Cluster. However, this signal, also detected by *Fermi*-LAT (Abdo et al. 2009), is consistent with an emission from the giant elliptical galaxy NGC 1275 lying at its centre (Aleksić et al. 2010, 2012). From the *Fermi*-LAT results, Colafrancesco et al. (2010) argue that it should be possible to resolve and detect the diffuse γ-ray flux of astrophysical origin coming from the outer corona of the Perseus cluster. Even more recently, Han et al. (2012) reported a detection for Virgo, Fornax, and Coma from an analysis of *Fermi*-LAT data. These authors find that an interpretation in terms of DM annihilation is preferred by their analysis, although a CR origin is also possible.

From these promising results, we anticipate that many clusters will be detected with the current or the next generation of γ-ray instruments. Multi-wavelength analyses, search for a spectral feature, and angular dependence of the signal are tests to disentangle γ-rays of astrophysical or DM origin. In this paper, we investigate another test based on the study of a population of sources, thus somehow positioned between single source and full sky power-spectrum analyses (Ando & Komatsu 2006). Actually, several studies have compared the astrophysical and

DM annihilation signal (Jeltema et al. 2009; Pinzke et al. 2011) as well as DM annihilation and decay (Huang et al. 2012) on a somewhat limited number of clusters (due to the size of the available catalogues at the time). However, the systematic study of the prospects of a stacking analysis with respect to single-source analyses has not been investigated before.

This paper is part of an ongoing effort to address this question in the context of the recently assembled MCXC meta-catalogue of 1743 X-ray clusters (Piffaretti et al. 2011). A first paper in this series highlighted the potential improvement (a factor $\gtrsim 5$–100) that can be brought by a stacking analysis over a single-source analysis for the DM decay case (Combet et al. 2012). A second paper considered the DM annihilation case in the light of the sensitivity of existing and future γ-ray instruments (Nezri et al. 2012). It showed that stacking only brings a factor of ~ 2 improvement in sensitivity for the *Fermi*-LAT instrument, but no improvement for Cherenkov Telescope Array (CTA)-like observatories. This third and last paper of the series inspects the case of the CR signal to address the possibility of using a stacking strategy to disentangle it from DM-induced signals. For that purpose, we use a generic description of the CR signal and refer the reader to the two previous papers (Combet et al. 2012; Nezri et al. 2012) for a detailed description of the DM modelling. We stress that this study remains at the phenomenological level. We are waiting either for the detection of several objects or a better knowledge of the input ingredients in order to quantify further the potential of the new diagnosis we investigate.

We present the ingredients and the calculation in Sect. 2. We then present the results in Sect. 3 and conclude in Sect. 4.

2. Ingredients and calculation

The total flux expected in a given direction (l, b) (Galactic coordinates) and integrated over the solid angle $\Delta\Omega$ is given by the product of an energy-dependent term with an astrophysical term $\mathcal{A}$[1],

$$\frac{\mathrm{d}\phi(E, l, b, \Delta\Omega)}{\mathrm{d}E} = \frac{\mathrm{d}N}{\mathrm{d}E}(E) \times \mathcal{A}(l, b, \Delta\Omega). \qquad (1)$$

In this study, we discard the spectral term and focus on $\mathcal{A}$, which encodes all the information about the spatial dependence of the signal, and the relative intensity between clusters. $\mathcal{A}$ will be termed "flux" in the following, but should be understood as the astrophysical contribution to the actual γ-ray flux. For an observation in the direction of the cluster's centre (l_{cl}, b_{cl}) and using an integration angle α_{int},

$$\mathcal{A}_X(\alpha_{int}) \equiv \mathcal{A}_X(l_{cl}, b_{cl}, \Delta\Omega) = \int_{\Delta\Omega} \int \mathcal{E}_X(l', \Omega)\, \mathrm{d}l'\mathrm{d}\Omega \qquad (2)$$

is the integral of the "emissivity" $\mathcal{E}_X(l', \Omega)$, over line of sight l' and solid angle $\Delta\Omega = 2\pi \cdot (1 - \cos(\alpha_{int}))$ for the process X. For DM, $\mathcal{E}_{Decay} = \rho_{DM}$ for decay and $\mathcal{E}_{Annihil.} = \rho_{DM}^2$ for annihilation, where ρ_{DM} is the DM density profile in the galaxy cluster, as presented in Sect. 2.1. For CR, $\mathcal{E}_{CR} = C_{CR}$, as defined in Sect. 2.2.

---

[1] The redshift distribution of the MCXC catalogue of galaxy clusters (Piffaretti et al. 2011) peaks at $z \sim 0.1$ (see their Fig. 1). Following Combet et al. (2012) and Nezri et al. (2012), we neglect the absorption for the MCXC galaxy clusters, so that the energy-dependent term and the spatial term are decoupled.

The integral Eq. (2) is computed for all MCXC clusters with the CLUMPY[2] code v2011.09 (Charbonnier et al. 2012) adapted to include the CR-induced γ-ray case described below.

2.1. Dark matter halos

The DM distribution for each galaxy cluster is parametrised from (see Combet et al. 2012 for more details):

- its M_{500} value[3] provided in the MCXC catalogue (Piffaretti et al. 2011);
- the choice of a universal DM profile, here the widely used NFW profile (Navarro et al. 1997),

$$\rho_{NFW}(r) = \frac{\rho_s}{\left(\frac{r}{r_s}\right)\left(1 + \frac{r}{r_s}\right)^2}, \qquad (3)$$

where r_s is the scale radius and ρ_s is the normalisation;
- a mass-concentration relationship, where the concentration is defined to be $c_\Delta \equiv R_\Delta/r_s$ for an NFW profile[4]. The latter is observationally constrained at the cluster scale (Pointecouteau et al. 2005; Buote et al. 2007; Ettori et al. 2010), and it has also been extensively studied in numerical simulations (Wechsler et al. 2002, 2006; Zhao et al. 2003, 2009; Neto et al. 2007; Gao et al. 2008, 2011; Macciò et al. 2008; Duffy et al. 2008, 2010; Giocoli et al. 2010; Muñoz-Cuartas et al. 2011; Klypin et al. 2011). In this study, we use the parametrisation of Duffy et al. (2008).

For DM annihilation, we also have to take into account the contribution from substructures as they have been shown to boost the signal. In this work, we assume the following for the mass and spatial distribution of the substructures: i) $\mathrm{d}N_{subs}/\mathrm{d}M \propto M^{-\alpha_M}$ with $\alpha_M = 1.9$, a mass fraction $f_{DM} = 10\%$ in substructures (Springel et al. 2008), a minimal and maximal mass of $10^{-6}\, M_\odot$ and $10^{-2}\, M_{cluster}$ respectively, and the Bullock et al. (2001) concentration (down to the minimal mass); ii) the substructure spatial distribution $\mathrm{d}N_{subs}/\mathrm{d}V$ follows the host halo smooth profile. Recent high-resolution numerical simulations that are for Galaxy-like objects (Springel et al. 2008) or are dedicated to cluster-size halos (Gao et al. 2012b) provide different figures for the slope α_M, the mass fraction f_{DM}, and the spatial distribution of substructures. We will briefly comment on how other choices impact on our analysis[5].

2.2. Cosmic-ray component

High-energy γ-rays can also be produced from astrophysical processes, in particular from the interaction of cosmic-ray protons with the gas of the cluster. Pinzke & Pfrommer (2010) found a universal radial dependence of the emissivity $\mathcal{E}_{CR} \equiv C_{CR}(r)$ of the clusters based on cosmological simulations. These authors acknowledge, however, that the CR spatial distribution

---

[2] http://lpsc.in2p3.fr/clumpy/

[3] M_Δ (with $\Delta = 200$ or 500) is the mass enclosed in a sphere of radius R_Δ, the radius within which the average density reaches Δ times the critical density of the Universe.

[4] In practice, we work with virial quantities (see, e.g. Giocoli et al. 2010, to switch from Δ to virial quantities), e.g. R_{vir} is the physical size of the galaxy cluster halo.

[5] A detailed discussion of the annihilation signal and its dependence on the substructure parameters can be found in Sect. 3.4 of Nezri et al. (2012) and is not repeated here. We underline that taking the same distribution as the smooth halo for this quantity or using that of Gao et al. (2012b) does not impact the annihilation results (see Nezri et al. 2012).

from which γ-rays are emitted could be affected by, e.g. additional CRs injected from AGN, or CR diffusion in momentum and space. For instance, Enßlin et al. (2011) argue that merging clusters should have a more centrally concentrated CR population than relaxed ones, providing bi-modality of their γ-ray emissivities. Nevertheless, we limit ourselves to the simplest case and assume a universal dependence across the cluster population we study here. We follow the formalism from Pinzke & Pfrommer (2010) and Pinzke et al. (2011):

$$C_{\mathrm{CR}}(r) = \left\{ \frac{c_{200} - 5 \times 10^{-7}}{1 + \left(\frac{r}{R_{\mathrm{trans}}}\right)^{-b}} + 5 \times 10^{-7} \right\} \times \rho_{\mathrm{gas}}^2(r), \qquad (4)$$

$$c_{200} = 1.7 \times 10^{-7} \left(\frac{M_{200}}{10^{15} \, M_\odot}\right)^{0.51}, \quad b = 1.04 \left(\frac{M_{200}}{10^{15} \, M_\odot}\right)^{0.15},$$

and $R_{\mathrm{trans}} = 0.021 \, R_{200} \left(\frac{M_{200}}{10^{15} \, M_\odot}\right)^{0.39}$.

Similar to the X-ray luminosity, the γ-ray emissivity is proportional to the square of the gas density $\rho_{\mathrm{gas}}^2(r)$. It is thereby very sensitive to the densest central parts of clusters. The relation between the DM and $\rho_{\mathrm{gas}}(r)$ has been extensively studied from a theoretical point of view (Makino et al. 1998; Suto et al. 1998; Komatsu & Seljak 2001; Ostriker et al. 2005; Bode et al. 2009; Frederiksen et al. 2009; Capelo et al. 2012). From the REXCESS representative sample, Croston et al. (2008) showed the universal behaviour of $\rho_{\mathrm{gas}}(r)$ in clusters (though a large scatter exists at the centre). The AB model, first introduced by Pratt & Arnaud (2002), and given by

$$\rho_{\mathrm{gas}}(x) \propto \left(\frac{x}{x_c}\right)^{-k_1} \left[1 + \left(\frac{x}{x_c}\right)^2\right]^{-3k_2/2 + k_1/2} \qquad (5)$$

with $x \equiv r/R_{500}$, was fitted to the average REXCESS density profile by Arnaud et al. (2010), with best-fit parameters $x_c = 0.303$, $k_1 = 0.525$, and $k_2 = 0.768$. This analytical phenomenological model reproduces well the cuspy shape of density profiles derived from X-ray observations and was also used for the MCXC assembly (Piffaretti et al. 2011). In order to remain consistent with respect to the data we use, the same AB profile is used here. The normalisation of Eq. (5) is chosen to give $f_{\mathrm{gas}} M_{500}$ at R_{500}. From the MCXC masses M_{500} and the empirical relation between f_{gas} and M_{500} given for the REXCESS sample (Pratt et al. 2009), an average value of $f_{\mathrm{gas}} = 0.10 \pm 0.06$ is derived, which we use for the whole MCXC sample. We note that the gas fraction increases with radius in halos (to ultimately tends towards the cosmic value), and the intrinsic scatter is important and scales with the cluster mass (Vikhlinin et al. 2006; Ettori et al. 2009; Pratt et al. 2009, 2010).

3. Results

We first comment on the universality of the γ-ray signal angular dependence. In particular, we inspect whether this universality holds for any signal hypothesis (annihilating DM, decaying DM, or CRs); in that case, observations of different objects may be optimally stacked to increase the signal. We also inspect whether a given angular dependence can be associated to a unique signal origin. We then turn to the comparison of the galaxy cluster population signals.
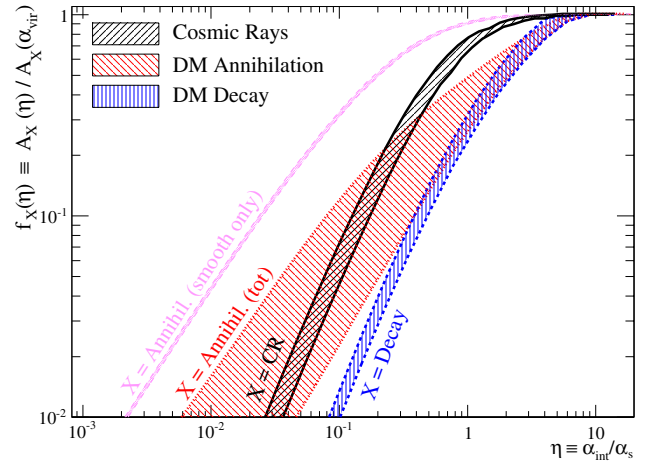

Fig. 1. Signal fraction $f_X(\eta)$ (for process X) as function of the reduced integration angle $\eta \equiv \alpha_{\mathrm{int}}/\alpha_s$. For the sake of presentation, only the envelopes for the 1743 clusters of the catalogue are shown. For annihilation, the signal for the smooth only is also shown (the substructure contribution only is similar to the decay case).

3.1. A different angular dependence for different origins?

The spatial dependence of the signal has been suggested as a test to disentangle DM decay from annihilation, in particular in dSphs (Palomares-Ruiz & Siegal-Gaskins 2010). Indeed, the use of universal DM profiles ensures that the projected profiles are universal if properly normalised by their value at $r = r_s$. By construction, the projected profiles for decay are universal, and so they are for annihilation if the smooth signal only is taken into account. However, as can be deduced from Gao et al. (2012a) results and as underlined in Nezri et al. (2012), the substructure contribution overtakes the smooth contribution at various distances from the centre, depending on the mass of the object rather than on its scale radius. Small objects (like dSphs) are dominated by their smooth contribution up to large distances from their centre, whereas massive galaxy clusters are almost completely dominated by the substructure contribution. As a result, departure from universality of the total DM annihilation signal (the one which we have access to) is expected.

This is illustrated using all MCXC galaxy clusters. Defining for any cluster its virial angle $\alpha_{\mathrm{vir}} = \tan^{-1}(R_{\mathrm{vir}}/d)$ and its scale angle $\alpha_s = \tan^{-1}(rs/d)$ (d its distance to the observer), we show in Fig. 1 the fraction of the integrated signal with respect to the maximal signal obtained, i.e.

$$f_X(\eta) \equiv \frac{\mathcal{A}_X(\alpha_{\mathrm{int}} = \eta \cdot \alpha_s)}{\mathcal{A}_X(\alpha_{\mathrm{vir}})} \qquad (6)$$

as a function of $\eta = \alpha_{\mathrm{int}}/\alpha_s$.

For DM annihilation, the smooth contribution (left-hand envelope) is the most centrally concentrated as it comes from the integration of the steep DM profile squared ($\rho_{\mathrm{DM}}^2 \xrightarrow{r \to 0} r^{-2}$).

For the decay signal (right-hand envelope), the external parts of the halo contribute more significantly to the signal because the quantity to integrate is shallower ($\rho_{\mathrm{DM}} \xrightarrow{r \to 0} r^{-1}$). We note that in the MCXC catalogue, the mass ratio of the most massive galaxy cluster to the least massive one is ~100, so that these clusters have different concentrations R_{vir}/r_s, hence a different rescaled angular size $\alpha_{\mathrm{vir}}/\alpha_s$. It does not impact on the DM annihilation signal from the smooth halo (because this signal is strongly centrally concentrated), but it leads to a small spread for a decay-like

signal. We checked that using an Einasto profile (Springel et al. 2008) instead of a NFW for the DM halos does not change the curves significantly.

For CRs (black envelope), the trend is similar to the decay case because $\rho_{gas}^2 \xrightarrow{r \to 0} r^{-1.05}$. The shift between the CRs and decay envelopes comes from the gas being more centrally concentrated than DM.

The DM annihilation from substructures is directly proportional to the integration of the substructure spatial distribution dN_{subs}/dV, which we have chosen in this work to follow the smooth DM profile. Because of this choice, the signal from substructures follows the same dependence as DM decay and is therefore not repeated in the figure. Similar to the smooth annihilation signal, changing this distribution does not impact on the conclusions significantly. As underlined, the more complex (i.e. non-universal) scaling of the total annihilation signal shown in Fig. 1 comes from the fact that both the smooth halo and the substructures contribute to the signal. As shown in Fig. 4 of Nezri et al. (2012), the distribution of boosts for the MCXC sample depends on the substructure configuration, and it can vary from 1 (no boost) to about 100 for a Phoenix-like configuration. In the former case, the angular dependence would be close to the smooth only annihilation case, whereas for the latter case, it would show a decay-like angular dependence.

To conclude, whereas the angular dependence is sometimes argued to be a good diagnosis to disentangle a CR signal from a DM signal, we draw attention to the fact that the situation is not that clear cut for galaxy clusters. Indeed, a CR signal is more centrally concentrated than a DM decay signal. However, for the annihilation case, it could be more concentrated than the CR signal, close to the DM decay case, or in-between.

3.2. Number of objects per flux bin

We now turn to the behaviour of the number of objects found given their flux, i.e. the $\log N - \log F$ dependence, where $F \propto \mathcal{A}_X$ is the actual observed flux (it is referred to as the $\log N - \log \mathcal{A}_X$ dependence below). Let us define the relative flux $\bar{A}_X^i$ of the ith galaxy cluster, i.e. the flux relative to that of the brightest object of the catalogue for the process X at stake:

$$\bar{A}_X^i \equiv \frac{\mathcal{A}_X^i}{\mathcal{A}_X^{brightest}}. \qquad (7)$$

Such a definition allows us to visually compare the behaviour for the different X processes.

This is shown in Fig. 2, where the number of objects N per logarithmic bin (of $\bar{A}_X$) is plotted for the MCXC sample. At first glance, the value of the slope s ($N \propto \bar{A}_X^{-s} \propto \mathcal{A}_X^{-s}$) in the region beyond the distribution peak can be used as a diagnosis of the signal origin[6]. We observe that the behaviour of the DM annihilation and CR components is very similar. This is tentatively explained by the fact that the CR emissivity Eq. (4) is $\propto \rho_{gas}^2 \propto M^2$ and DM annihilation is $\propto \rho_{DM}^2$. For the latter, the slope $s_{annihil.}$ varies in the range $[s_{decay}/2, \; s_{decay}]$: for small integration angles (top left), $\mathcal{E}_{decay} \propto \rho_{DM}$ and $\mathcal{E}_{annihil} \propto \rho_{DM}^2$ and $s_{annihil.} \approx s_{decay}/2$ (substructures scarcely play a role in the central regions of the cluster), whereas for integration angles encompassing the whole cluster (bottom right), the substructure

[6] The catalogue is not complete across the range of masses it samples, explaining the peaks seen in Fig. 2 (the selection function is undetermined, beyond the scope of this paper, and not accounted for in the discussion).
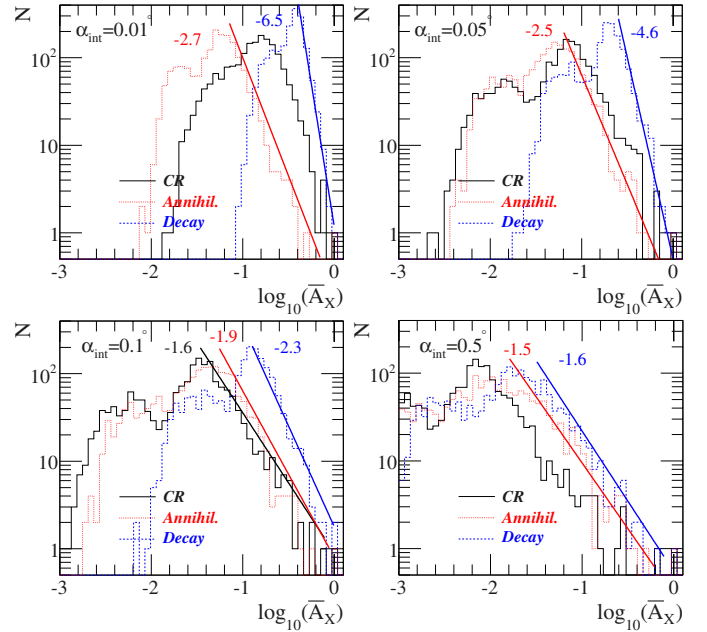
Fig. 2. Number of galaxy clusters per logarithmic bin of $\bar{A}_X$ (see Eq. (7)), for the CR component (solid black), DM annihilation (dotted red), and DM decay (dashed blue). The four panels correspond to four integration angles α_{int} (from *top left to bottom right*, 0.01°, 0.05°, 0.1°, and 0.5°). The index s of the power law $N \propto \mathcal{A}^s$ fit is shown for $\alpha_{int} = 0.1°$ for the three components.

contribution becomes dominant and $s_{annihil.} \approx s_{decay}$. Actually, the annihilation signal at any given integration angle is sensitive to the DM substructure configuration (as explained in the previous section, see also Sect. 3.4 of Nezri et al. 2012), so that the values of $s_{annihil.}$ shown in Fig. 2 are very uncertain (they are bracketed by the value obtained for the CR case and the value for the decay case).

The actual value of s is difficult to explain from simple arguments because it comes from the interplay of the profile, normalisation, and integration angle for each cluster. This analysis nevertheless shows that a CR origin can be disentangled from a DM origin in the case of a decaying DM candidate.

3.3. Stacked signal

As deduced from Fig. 3, the ratio between the brightest and next-to-brightest clusters could also be an indicator of the γ-ray signal origin (it is the largest for CR origin and the lowest for decay at 0.5°, bottom right-hand panel). This is, however, sensitive to the individual modelling of the clusters, especially for the annihilation case because of the extra uncertainty from DM substructures. In that respect, this ratio criterion (or also using the ratio of the CR signal to the DM annihilation signal, see Pinzke et al. 2011) should be used with caution. The cumulative[7] of the signal also suffers from similar uncertainties. However, as the number of stacked objects increases, the sensitivity to the modelling of a given halo becomes less crucial. The possibility to identify the origin X of a signal from the behaviour of the stacked signal is very similar in spirit to comparing the slope s of the $\log N - \log \mathcal{A}_X$ relation. However, if the signal is only seen by means of stacking, it may not be possible to get s, but still possible to say something about the origin from this detection.

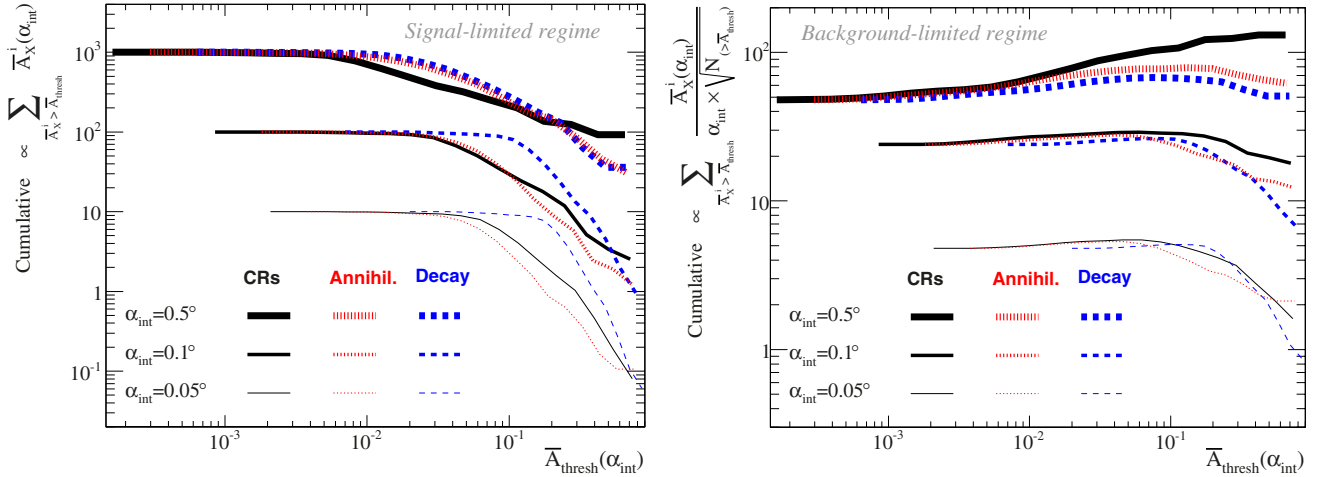[7] The cumulative is defined to be the cumulated flux of all objects brighter than a threshold flux.

Fig. 3. Cumulative of the signal above a threshold value $\bar{A}_{\text{thresh}}$ for the signal-limited regime (*left panel*, corresponding to Eq. (8)) and for the background-limited regime (*right panel*, corresponding to Eq. (9)). The three line widths correspond to three integration angles, and the three styles and colours correspond to CRs, DM annihilation, and decay. An arbitrary normalisation is set in order to ease the comparison by eye of the different signals.

The promise of a stacking analysis for a signal X depends on the slope s of the $\log N - \log \mathcal{A}_X$ relation. If the number of objects increases faster than the signal decreases, a better sensitivity should be reached compared to the single-source analysis case. This was shown to be the case for decay in Combet et al. (2012), but not for annihilation (Nezri et al. 2012). A detailed discussion of detectability in the light of the *Fermi*-LAT and CTA-like instruments was also presented in that paper. Here, we extend the analysis to the CR case, and comment on the differences between the various signals. The simple approach used in Combet et al. (2012) is enough to capture the trends and draw some conclusions, i.e. we consider the generic extreme case of a signal- and a background-limited observation[8].

As in the previous section, we work with the normalised flux $\bar{A}_X$ defined by Eq. (7) to ease the comparison between the different X origins. The cumulative for a signal-limited observation (left-hand panel) corresponds to

$$\mathcal{K}_{\text{Sig-lim}}(\alpha_{\text{int}}) \propto \sum_{\bar{A}_X^i > \bar{A}_{\text{thresh}}} \bar{A}_X^i(\alpha_{\text{int}}), \tag{8}$$

while that for a background-limited observation is

$$\mathcal{K}_{\text{Bkgd-lim}}(\alpha_{\text{int}}) \propto \frac{\mathcal{K}_{\text{Sig-lim}}(\alpha_{\text{int}})}{\alpha_{\text{int}} \sqrt{N_{(>\bar{A}_{\text{thresh}})}}}, \tag{9}$$

where $N_{(>\bar{A}_{\text{thresh}})}$ is the number of clusters satisfying $\bar{A}_X^i(\equiv \mathcal{A}_X^i / \mathcal{A}_X^{\text{brightest}}) > \bar{A}_{\text{thresh}}$. This is shown in Fig. 3 for the MCXC catalogue[9]. For display purposes, the curves for various processes X are normalised to the asymptotic value (when all objects are stacked), whereas the curves for different integration angles α_{int} are shifted from one another.

Regardless of the integration angle and whether the regime is signal or background limited, stacking leads to a significantly

larger increase of the signal for DM decay than for the CR case. Indeed, as shown in Combet et al. (2012) for the DM decay component, improvement with respect to the brightest source can reach at best (with the MCXC catalogue) a factor of ∼100 for background-free instruments, but a factor ∼5 is expected for more realistic background-limited instruments. For both the CR and DM annihilation component, the improvement is respectively ∼50 (background free) and ∼2 (background limited) for $\alpha_{\text{int}} \lesssim 0.1°$. A detailed analysis based on a realistic instrumental response for the *Fermi*-LAT and CTA instruments shows that this factor of two (for annihilation) is only achieved for *Fermi*-LAT, there is no improvement with CTA-like instruments (Nezri et al. 2012). Hence a similar result is expected for the CR-induced origin. Although in principle the behaviour of stacked signals at different angles for the DM annihilation case can be disentangled from the two other cases for the signal-limited regime, the uncertainties on the substructure distribution are such that the spread generated on the stacked annihilation signal is encompassed by the CR and DM decay case and thus cannot be distinguished for now.

4. Conclusion

The first two papers of this series investigated the potential benefit of a stacking analysis of clusters of galaxies for DM detection. Relying on the largest uniformed X-ray catalogue to date, the MCXC catalogue (Piffaretti et al. 2011), it was shown that a DM decay signal benefits from a stacking analysis (Combet et al. 2012), but that the situation is less promising for the annihilation signal (Nezri et al. 2012). In this third and last paper of the series, we extended the analysis to the expected CR-induced component, hoping to put to the forth a difference that may be used as a novel diagnosis to identify the origin of the signal when detection in such objects becomes routinely available.

Based on the slope s of the $\log N - \log \mathcal{A}_X$ behaviour (or equivalently on the benefit gained by stacking the signal from many objects), we have found that a DM origin can be identified against an astrophysical background in the case of decaying DM, but not for annihilating DM. Though, in principle, combining the angular-dependence information and the stacked signal at different integration angles gives clues as to the signal origin, the

---

[8] The detectability of galaxy clusters depends both on the integrated signal and on the much higher level of charged particle and diffuse astrophysical γ-ray backgrounds. In the background-limited regime the best approach is to maximise the signal-to-noise ratio. For a uniform background, it corresponds to the cumulative of $\mathcal{A}_X$ divided by the square root of the background which is $\propto \alpha_{\text{int}}^2 N$.

[9] The plateau reached by the cumulative signal on the left-hand panel is due to the drop of the number of objects seen in Fig. 2.

existing uncertainties on the DM substructures (which may contribute significantly to the annihilation signal) prevents us from reaching any clear conclusion. Furthermore, whereas it has been sometimes argued that the angular dependence can be used to disentangle DM decay from DM annihilation, we have shown for galaxy clusters that i) there is not strictly a universal angular dependence for the annihilating signal, and ii) that the very uncertainties on the DM substructures prevent us from predicting exactly what this dependence is. Hence, decaying DM is the simplest scenario to test and/or exclude, because it is the most sensitive to stacking and the angular dependence of several objects can also be stacked (with a rescaling).

The robustness of this analysis would benefit from a more thorough investigation that takes into account various sources of uncertainties, such as the DM and gas profile modelling. For instance, the intrinsic scatter observed in gas density profiles at the centre of clusters (due to gas physics, interactions with the central galaxy and with the often present active nucleus, the dynamical state of the cluster, etc.) could affect the CR signal signature. Similarly a more systematic check of the dependence of the DM annihilation signal on the clump parameters (for the substructures' contribution) is certainly needed. The calculations presented here have been done in the idealised scenario where all clusters have a dominant signal component of the same nature, whether it be DM decay, annihilation or astrophysical. The effect may be even less clear if this is not the case. Nevertheless, this may be a useful test that will complement those already suggested in the literature (spectral feature, spatial-dependence of the signal, multi-wavelength analysis, angular power spectrum).

References

Abdo, A. A., Ackermann, M., Ajello, M., et al. 2009, ApJ, 699, 31
Ackermann, M., Ajello, M., Allafort, A., et al. 2010, ApJ, 717, L71
Aharonian, F., Akhperjanian, A. G., Aye, K.-M., et al. 2004, A&A, 425, L13
Aharonian, F., Akhperjanian, A. G., Anton, G., et al. 2009a, A&A, 495, 27
Aharonian, F., Akhperjanian, A. G., Anton, G., et al. 2009b, A&A, 502, 437
Aleksić, J., Antonelli, L. A., Antoranz, P., et al. 2010, ApJ, 710, 634
Aleksić, J., Alvarez, E. A., Antonelli, L. A., et al. 2012, A&A, 539, L2
Ando, S., & Komatsu, E. 2006, Phys. Rev. D, 73, 023521
Ando, S., & Nagai, D. 2012, J. Cosmol. Astropart. Phys., 7, 17
Arnaud, M., Pratt, G. W., Piffaretti, R., et al. 2010, A&A, 517, A92
Bode, P., Ostriker, J. P., & Vikhlinin, A. 2009, ApJ, 700, 989
Bringmann, T., Calore, F., Vertongen, G., & Weniger, C. 2011, Phys. Rev. D, 84, 103525
Bullock, J. S., Kolatt, T. S., Sigad, Y., et al. 2001, MNRAS, 321, 559
Buote, D. A., Gastaldello, F., Humphrey, P. J., et al. 2007, ApJ, 664, 123
Capelo, P. R., Coppi, P. S., & Natarajan, P. 2012, MNRAS, 422, 686
Charbonnier, A., Combet, C., & Maurin, D. 2012, Comput. Phys. Commun., 183, 656

Colafrancesco, S., Profumo, S., & Ullio, P. 2006, A&A, 455, 21
Colafrancesco, S., Marchegiani, P., & Giommi, P. 2010, A&A, 519, A82
Combet, C., Maurin, D., Nezri, E., et al. 2012, Phys. Rev. D, 85, 063517
Croston, J. H., Pratt, G. W., Böhringer, H., et al. 2008, A&A, 487, 431
Duffy, A. R., Schaye, J., Kay, S. T., & Dalla Vecchia, C. 2008, MNRAS, 390, L64
Duffy, A. R., Schaye, J., Kay, S. T., et al. 2010, MNRAS, 405, 2161
Enßlin, T., Pfrommer, C., Miniati, F., & Subramanian, K. 2011, A&A, 527, A99
Ettori, S., Morandi, A., Tozzi, P., et al. 2009, A&A, 501, 61
Ettori, S., Gastaldello, F., Leccardi, A., et al. 2010, A&A, 524, A68
Frederiksen, T. F., Hansen, S. H., Host, O., & Roncadelli, M. 2009, ApJ, 700, 1603
Gao, L., Navarro, J. F., Cole, S., et al. 2008, MNRAS, 387, 536
Gao, L., Frenk, C. S., Boylan-Kolchin, M., et al. 2011, MNRAS, 410, 2309
Gao, L., Frenk, C. S., Jenkins, A., Springel, V., & White, S. D. M. 2012a, MNRAS, 419, 1721
Gao, L., Navarro, J. F., Frenk, C. S., Jenkins, A., Springel, V., & White, S. D. M. 2012b, MNRAS, 425, 2169
Giocoli, C., Tormen, G., Sheth, R. K., & van den Bosch, F. C. 2010, MNRAS, 404, 502
Han, J., Frenk, C. S., Eke, V. R., Gao, L., & White, S. D. M. 2012 [arXiv:1201.1003]
Huang, X., Vertongen, G., & Weniger, C. 2012, J. Cosmol. Astropart. Phys., 1, 42
Jeltema, T. E., & Profumo, S. 2011, ApJ, 728, 53
Jeltema, T. E., Kehayias, J., & Profumo, S. 2009, Phys. Rev. D, 80, 023005
Kiuchi, R., Mori, M., Bicknell, G. V., et al. 2009, ApJ, 704, 240
Klypin, A. A., Trujillo-Gomez, S., & Primack, J. 2011, ApJ, 740, 102
Komatsu, E., & Seljak, U. 2001, MNRAS, 327, 1353
Macciò, A. V., Dutton, A. A., & van den Bosch, F. C. 2008, MNRAS, 391, 1940
Makino, N., Sasaki, S., & Suto, Y. 1998, ApJ, 497, 555
Muñoz-Cuartas, J. C., Macciò, A. V., Gottlöber, S., & Dutton, A. A. 2011, MNRAS, 411, 584
Navarro, J. F., Frenk, C. S., & White, S. D. 1997, ApJ, 490, 493
Neto, A. F., Gao, L., Bett, P., et al. 2007, MNRAS, 381, 1450
Nezri, E., White, R., Combet, C., et al. 2012, MNRAS, 425, 477
Ostriker, J. P., Bode, P., & Babul, A. 2005, ApJ, 634, 964
Palomares-Ruiz, S., & Siegal-Gaskins, J. M. 2010, J. Cosmol. Astropart. Phys., 7, 23
Pato, M., Pieri, L., & Bertone, G. 2009, Phys. Rev. D, 80, 103510
Perkins, J. S., Badran, H. M., Blaylock, G., et al. 2006, ApJ, 644, 148
Piffaretti, R., Arnaud, M., Pratt, G. W., Pointecouteau, E., & Melin, J.-B. 2011, A&A, 534, A109
Pinzke, A., & Pfrommer, C. 2010, MNRAS, 409, 449
Pinzke, A., Pfrommer, C., & Bergström, L. 2011, Phys. Rev. D, 84, 123509
Pointecouteau, E., Arnaud, M., & Pratt, G. W. 2005, A&A, 435, 1
Pratt, G. W., & Arnaud, M. 2002, A&A, 394, 375
Pratt, G. W., Croston, J. H., Arnaud, M., & Böhringer, H. 2009, A&A, 498, 361
Pratt, G. W., Arnaud, M., Piffaretti, R., et al. 2010, A&A, 511, A85
Regis, M., & Ullio, P. 2008, Phys. Rev. D, 78, 043505
Springel, V., Wang, J., Vogelsberger, M., et al. 2008, MNRAS, 391, 1685
Suto, Y., Sasaki, S., & Makino, N. 1998, ApJ, 509, 544
Vikhlinin, A., Kravtsov, A., Forman, W., et al. 2006, ApJ, 640, 691
Walker, M. G., Combet, C., Hinton, J. A., Maurin, D., & Wilkinson, M. I. 2011, ApJ, 733, L46
Wechsler, R. H., Bullock, J. S., Primack, J. R., Kravtsov, A. V., & Dekel, A. 2002, ApJ, 568, 52
Wechsler, R. H., Zentner, A. R., Bullock, J. S., Kravtsov, A. V., & Allgood, B. 2006, ApJ, 652, 71
Zhao, D. H., Jing, Y. P., Mo, H. J., & Börner, G. 2003, ApJ, 597, L9
Zhao, D. H., Jing, Y. P., Mo, H. J., & Börner, G. 2009, ApJ, 707, 354